Main Equations of Wang's Anand-Type Viscoplastic Model

Flow Rule (Plastic Strain Rate)

- $$\dot{\varepsilon}^p = A \exp\left(-\frac{Q}{RT}\right)\left[\sinh\left(\frac{j\sigma}{s}\right)\right]^{1/m}$$
- Plastic strain rate increases with stress and temperature.
- No explicit yield surface; flow occurs at all nonzero stresses.

Deformation Resistance Saturation s^*

- $$s^* = \hat{s}\left(\frac{\dot{\varepsilon}^p}{A}\exp\left(\frac{Q}{RT}\right)\right)^n$$
- Defines the steady-state value that s evolves toward.
- Depends on strain rate and temperature.

Evolution of Deformation Resistance s

- $$\dot{s} = h_0\left|1 - \frac{s}{s^*}\right|^a \operatorname{sign}\left(1 - \frac{s}{s^*}\right)\dot{\varepsilon}^p$$
- Describes dynamic hardening and softening of the material.
- s evolves depending on proximity to s^* and flow activity.

Note: Constants $A, Q, m, j, h_0, \hat{s}, n, a$ are material-specific and fitted to experimental creep/strain rate data.

Multichamber Muffler System

Michael Raba, MSc Candidate at University of Kentucky

Created: 2025-09-15 Mon 14:27

Comparing Anand Model Predictions at Two Strain Rates

Observed Behavior

- **Top Graph (a):** $\dot{\varepsilon} = 10^{-2}\,\mathrm{s}^{-1}$
- High strain rate → higher stress
- Recovery negligible → pronounced hardening
- **Bottom Graph (b):** $\dot{\varepsilon} = 10^{-4}\,\mathrm{s}^{-1}$
- Lower strain rate → lower stress at same strain
- Recovery and creep effects more significant

Model Accuracy: Lines = model prediction, X = experimental data

Key Insights from Wang (2001)

- "At lower strain rates, recovery dominates… the stress levels off early."
- "At high strain rates, hardening dominates, and the stress grows continuously."

Anand's model smoothly captures strain-rate and temperature dependence of solder materials.

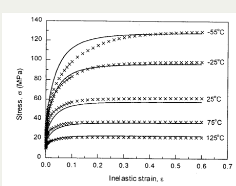

(a) $\dot{\varepsilon}$ =1.0×10^{-2} s^{-1}

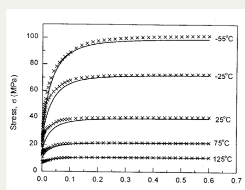

(b) $\dot{\varepsilon}$ =1.0×10^{-4} s^{-1}

Case Study: Wang (2001) Apply to Solder

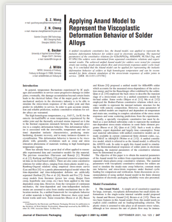

Applying Anand Model to Represent the Viscoplastic Deformation Behavior of Solder Alloys

G. Z. Wang, Z. N. Cheng, K. Becker, J. Wilde

Journal of Electronic Packaging

Source: Wang, C. H. (2001). "A Unified Creep–Plasticity Model for Solder Alloys."
DOI: 10.1115/1.1371781

Why Wang's Paper Matters

- Applies Anand's unified viscoplastic framework to model solder behavior.
- Anand's model can be reduced and fitted from experiments.
- transition the theory into engineering-scale implementation.
- Targets solder joints in microelectronic packages (chip on PCB, soldered connections).

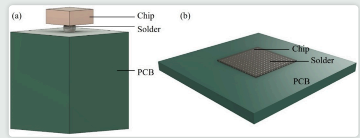

Multicomponent Muffler Internal Geometry

Dimensions

dimensional units in mm

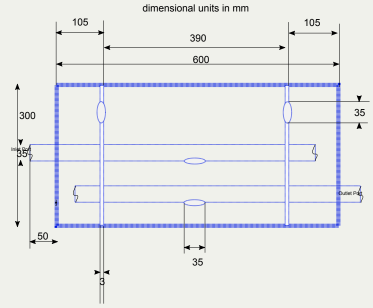

Source Paper

Constitutive Equations for Hot-Working of Metals

Author: Lallit Anand (1985)

DOI: 10.1016/0749-6419(85)90004-X

One of the foundational papers in thermodynamically consistent viscoplasticity modeling—especially significant in the context of metals subjected to large strains and high temperatures.

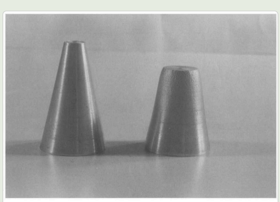

Fig. 25. 1100 aluminum state gradient specimens before and after testing.

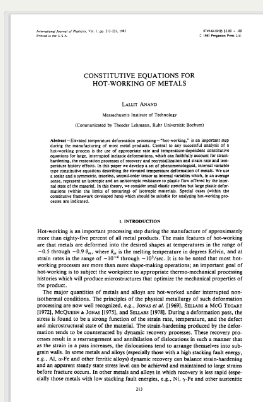

International Journal of Plasticity, Vol. 1, pp. 213–231, 1985
Printed in the U.S.A.
0749-6419/85 $3.00 + .00

CONSTITUTIVE EQUATIONS FOR HOT-WORKING OF METALS

Lallit Anand
Massachusetts Institute of Technology

(Communicated by Theoder Lehmann, Ruhr Universität Bochum)

Abstract—Elevated temperature deformation processing—"hot-working," is an important step during the manufacturing of most metal products. Central to any successful analysis of a hot-working process is the use of appropriate rate and temperature-dependent constitutive equations for large, interrupted inelastic deformations, which can faithfully account for strain-hardening, the restoration processes of recovery and recrystallization and strain rate and temperature history effects. In this paper we develop a set of phenomenological, internal variable type constitutive equations describing the elevated temperature deformation of metals. We use a scalar and a symmetric, traceless, second-order tensor as internal variables which, in an average sense, represent an isotropic and an anisotropic resistance to plastic flow offered by the internal state of the material. In this theory, we consider small elastic stretches but large plastic deformations (within the limits of texturing) of isotropic materials. Special cases (within the constitutive framework developed here) which should be suitable for analyzing hot-working processes are indicated.

I. INTRODUCTION

Hot-working is an important processing step during the manufacture of approximately more than eighty-five percent of all metal products. The main features of hot-working are that metals are deformed into the desired shapes at temperatures in the range of ~0.5 through ~0.9 θ_m, where θ_m is the melting temperature in degrees Kelvin, and at strain rates in the range of ~10^{-4} through ~10^3/sec. It is to be noted that most hot-working processes are more than mere shape-making operations; an important goal of hot-working is to subject the workpiece to appropriate thermo-mechanical processing histories which will produce microstructures that optimize the mechanical properties of the product.

The major quantities of metals and alloys are hot-worked under interrupted non-isothermal conditions. The principles of the physical metallurgy of such deformation processing are now well recognized, e.g., Jonas *et al.* [1969], Sellars & McG Tegart [1972], McQueen & Jonas [1975], and Sellars [1978]. During a deformation pass, the stress is found to be a strong function of the strain rate, temperature, and the defect and microstructural state of the material. The strain-hardening produced by the deformation tends to be counteracted by dynamic recovery processes. These recovery processes result in a rearrangement and annihilation of dislocations in such a manner that as the strain in a pass increases, the dislocations tend to arrange themselves into subgrain walls. In some metals and alloys (especially those with a high stacking fault energy, e.g., Al, α-Fe and other ferritic alloys) dynamic recovery can balance strain-hardening and an apparent steady state stress level can be achieved and maintained to large strains before fracture occurs. In other metals and alloys in which recovery is less rapid (especially those metals with low stacking fault energies, e.g., Ni, γ-Fe and other austenitic

213

Anand Model: Viscoelastoplasticity and its Application to Solder Joints

Michael Raba, MSc Candidate at University of Kentucky

Created: 2025-09-15 Mon 14:27

Schematic Variants for Muffler Subcomponents

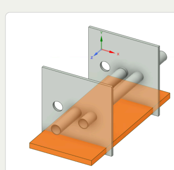

Part 1 — Chamber and Baffle

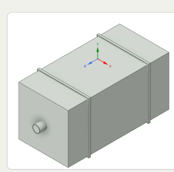

Part 2 — Fluid domain

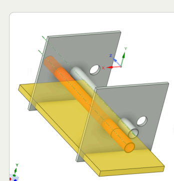

Part 3 — Fiberglass Absorbant (gold)

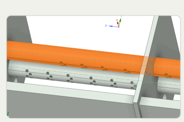

Part 4 — Showing perforates (aimed at fiberglass)

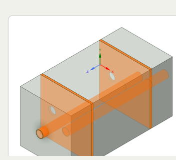

Part 5 — Final Assembly View

Ansys Simulation

Simulated Transmission Loss (0–1000 Hz) by approximating muffler walls as fluid at 20 deg C

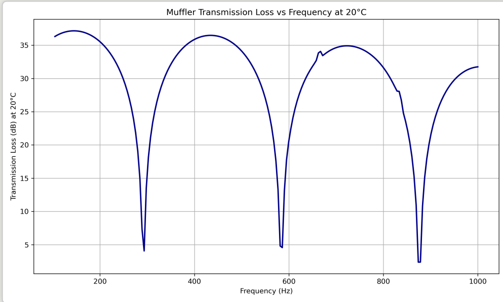

Figure: Transmission Loss curve of the muffler between 5 Hz and 1000 Hz at 20°C.

References

Cited Works

1. Munjal ML. *Acoustics of Ducts and Mufflers*. 2nd ed. Wiley; 2014. ISBN: 9781118443125. https://doi.org/10.1002/9781118443125
2. Dokumacı E. *Duct Acoustics: Fundamentals and Applications to Mufflers and Silencers*. Cambridge University Press; 2021. ISBN: 9781108840750. https://doi.org/10.1017/9781108840750

Note: These references are foundational texts in muffler and duct acoustics and were consulted for system modeling, schematic development, and transmission loss analysis.

Simulated vs Measured Insertion Loss

Measured vs Simulated TL

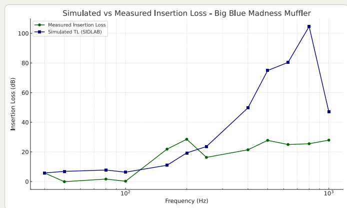

Insertion Loss Explanation

Insertion Loss (IL) quantifies how much sound is attenuated when a muffler is added to the system.

General formula:

$$\mathrm{IL} = 10\log_{10}\left(\frac{P_{\mathrm{baseline}}}{P_{\mathrm{muffler}}}\right)$$

Because our data is already in decibels (dB), this simplifies to:

$$\mathrm{IL} = \mathrm{Power}_{\mathrm{baseline\ (dB)}} - \mathrm{Power}_{\mathrm{muffler\ (dB)}}$$

Simlab Simulation

Simulated Transmission Loss (0–1000 Hz) Simlab model

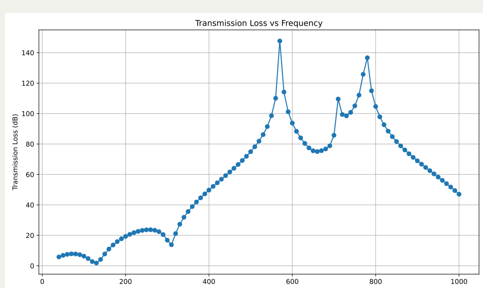

Sidlab and Ansys File Download Center

SIDLAB Model

- **File:** `Mark3Sid.zip`
- **Created with:** SIDLAB 5.1
- **⬇ Download SIDLAB File**

ANSYS Simulation

- **File:** `Mark-I-MDF-clearned-data.wbpz`
- **Created with:** ANSYS 2023 R2
- **⬇ Download ANSYS File**

Sidlab Components

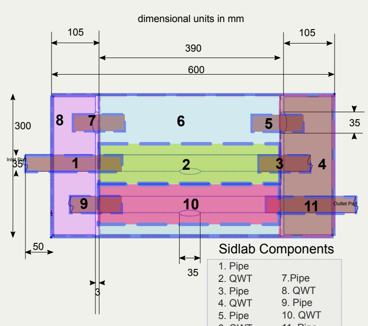

1. ↪ initPod.m
   - carries out POD calculations (quadrature, multiplication ggf betwen $\alpha\Phi$) according to Papers (Citriniti George 2000 for Classic POD, Hellstrom Smits 2017 for Snapshot POD)
2. ↪ timeReconstructFlow.m
   - performs 2d reconstruction + plotSkmr (generates 1d radial graph)

Anand Viscoplasticity Constants for 60Sn40Pb

Image Reference

Values are from correspond to 60Sn40Pb solder parameters used in Anand's model:

- S_0: Initial deformation resistance
- Q/R: Activation energy over gas constant
- A: Pre-exponential factor for flow rate
- ξ: Multiplier of stress inside sinh
- m: Strain rate sensitivity of stress
- h_0: Hardening/softening constant
- $\hat{s}$: Coefficient for saturation stress
- n: Strain rate sensitivity of saturation
- a: Strain rate sensitivity of hardening or softening

Numerical Values

- $S_0 = 5.633 \times 10^7$ Pa
- $Q/R = 10830$ K
- $A = 1.49 \times 10^7$ s^{-1}
- $\xi = 11$
- $m = 0.303$
- $h_0 = 2.6408 \times 10^9$ Pa
- $\hat{s} = 8.042 \times 10^7$ Pa
- $n = 0.0231$
- $a = 1.34$

These constants match Wang's paper for modeling 60Sn40Pb viscoplasticity.

Forward Euler Explicit time integration scheme Pseudocode

Initialization

- Material constants: $A, Q/R, j, m, h_0, \hat{s}, n, a, E$
- Strain rate: $\dot{\varepsilon}$
- Temperature set: $\{T_i\}$
- Set: $\varepsilon^p(0) = 0, \quad s(0) = \hat{s}$

Time Evolution Loop

1. $\varepsilon_{\text{total}}(t) = \dot{\varepsilon}\, t$
2. $\sigma_{\text{trial}} = E(\varepsilon_{\text{total}} - \varepsilon^p)$
3. Compute $x = \frac{j\sigma}{s}$
4. Approximate $\sinh(x)$ (linearize if $|x| \ll 1$)
5. $\dot{\varepsilon}^p = A e^{-Q/RT} (\sinh(x))^{1/m}$

Plastic Flow & Resistance Evolution

6. $s^* = \hat{s} \left(\frac{\dot{\varepsilon}^p}{A} e^{Q/RT} \right)^n$
7. $\dot{s} = h_0 \left| 1 - \frac{s}{s^*} \right|^a \text{sign}\left(1 - \frac{s}{s^*}\right) \dot{\varepsilon}^p$
8. Update: $\varepsilon^p(t + \Delta t) = \varepsilon^p(t) + \dot{\varepsilon}^p \Delta t$
9. Update: $s(t + \Delta t) = s(t) + \dot{s}\, \Delta t$
10. Record $(\varepsilon_{\text{total}}, \sigma_{\text{trial}})$

Termination

- Stop when $\varepsilon_{\text{total}} \geq \varepsilon_{\max}$
- Plot σ vs ε for all T_i

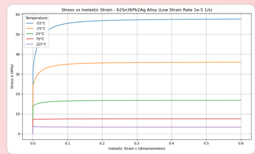

18

1.1. Layout

1. b7.m
2. initSpectral.m
   - reads in binary files, takes eg m-fft
3. ↪ initEigs.m
   - forms corrMat, finds eigenvalues

1. Code Execution and Layout

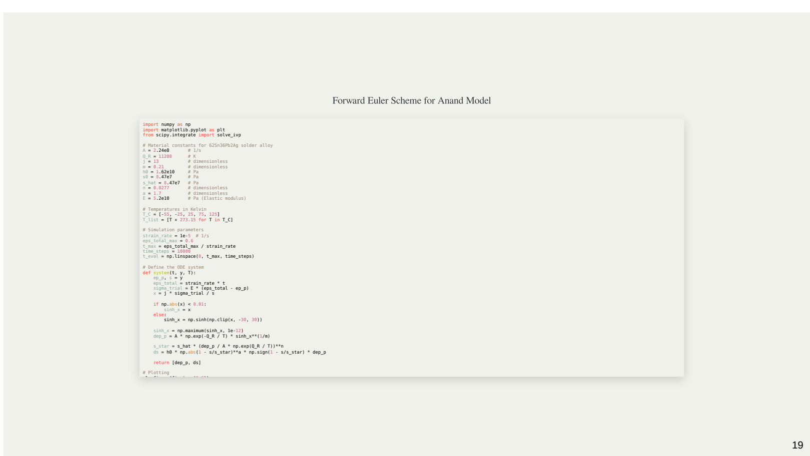

Strain rate sensitivity of stress m

- As $m \to 0$, rate insensitive (yield)
- As $m \to 1$, small stress change causes big change in strain rate

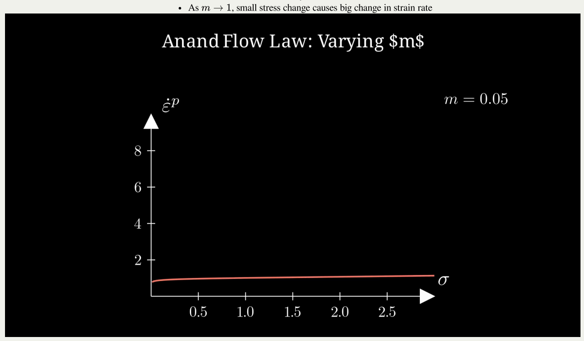

POD Analysis of Turbulent Pipe Flow

M. Raba

Created: 2025-09-15 Mon 14:27

Thermodynamic Quantities

- Free energy density:

$$\boxed{\psi = \epsilon - \theta\eta}$$

- Reduced dissipation inequality:

$$\boxed{\dot{\psi} + \eta\dot{\theta} - \rho^{-1}\mathbf{T} : \mathbf{L} + (\rho\theta)^{-1}\mathbf{q} \cdot \mathbf{g} \leq 0}$$

- State variables:

$$\{E^e, \theta, \bar{g}, \bar{\mathbf{B}}, s\}$$

with E^e as elastic strain and s as internal resistance.

Stress Power and Kirchhoff Stress

- Stress power per relaxed volume:

$$\boxed{\dot{\omega} = \left(\frac{\rho_0}{\rho}\right) \mathbf{T} : \mathbf{L}}$$

- Weighted Cauchy (Kirchhoff) stress:

$$\boxed{\widetilde{\mathbf{T}} = (\det F)\mathbf{T}} \quad \text{or} \quad \boxed{\widetilde{\mathbf{T}} = \left(\frac{\rho_0}{\rho}\right) \mathbf{T}}$$

- Decomposition of stress power:

$$\boxed{\dot{\omega} = \dot{\omega}^e + \dot{\omega}^p}$$

$$\dot{\omega}^e = \widetilde{\mathbf{T}} : \dot{E}^e, \quad \dot{\omega}^p = (C^e \widetilde{\mathbf{T}}) : \mathbf{L}^p$$

Summary:
- Free energy and dissipation govern thermodynamic consistency.
- Stress power naturally splits into elastic and plastic parts.
- Kirchhoff stress simplifies stress evolution accounting for volume changes.

Tensorial Flow Rule (directional form)

$$\mathbf{D}^p = \dot{\epsilon}^p \left(\frac{3}{2}\frac{\mathbf{T}'}{\bar{\sigma}}\right)$$

Equivalent Stress Definition

$$\bar{\sigma} = \sqrt{\frac{3}{2}\mathbf{T}' : \mathbf{T}'}$$

Plastic Strain Rate (magnitude form)

$$\dot{\epsilon}^p = A \exp\left(-\frac{Q}{R\theta}\right) \left[\sinh\left(\xi \frac{\bar{\sigma}}{s}\right)\right]^{1/m}$$

Full Flow Rule with Hyperbolic Sine

$$\mathbf{D}^p = A \exp\left(-\frac{Q}{R\theta}\right) \left[\sinh\left(\xi \frac{\bar{\sigma}}{s}\right)\right]^{1/m} \left(\frac{3}{2}\frac{\mathbf{T}'}{\bar{\sigma}}\right),$$

$$= \dot{\gamma}^p \left(\frac{\widetilde{\mathbf{T}}'}{2\bar{\tau}}\right), \quad \bar{\tau} = \left\{\frac{1}{2}\mathrm{tr}(\widetilde{\mathbf{T}}'^2)\right\}^{1/2}$$

Summary:
- Direction given by $\mathbf{T}'$.
- Magnitude determined by hyperbolic sine based on $\bar{\sigma}/s$.
- $\bar{\tau}$ represents the effective shear stress computed from deviatoric stress.
- $\bar{\sigma} = \sqrt{\frac{3}{2}\mathbf{T}' : \mathbf{T}'}$ is the von Mises Equivalent stress, but is formally defined without yield point
- Full flow = **direction × magnitude**.

Evolution Equation for the Stress

Stress Evolution Equation (Rate form of Hooke's Law)

$$\overset{\nabla}{\mathbf{T}} = \mathbb{L}\left[\mathbf{D} - \mathbf{D}^p\right] - \mathbf{\Pi}\dot{\theta}$$

(rate-form Hooke's law for finite deformation plasticity, with frame-indifference enforced through the Jaumann rate.)

Jaumann Rate Definition

$$\overset{\nabla}{\mathbf{T}} = \dot{\mathbf{T}} - \mathbf{W}\mathbf{T} + \mathbf{T}\mathbf{W}$$

Material Tensors and Operators

- $\mathbb{L} = 2\mu\mathbf{I} + \left(\kappa - \frac{2}{3}\mu\right)\mathbf{1} \otimes \mathbf{1}$ — isotropic elasticity tensor
- $\mathbb{L}\mathbf{D}$ represents how instantaneous strain rates generate stresses according to the elastic material's stiffness properties.
- $\mu = \mu(\theta)$, $\kappa = \kappa(\theta)$ — temperature-dependent moduli
- $\mathbf{\Pi} = (3\alpha\kappa)\mathbf{1}$ — stress-temperature coupling
- $\alpha = \alpha(\theta)$ — thermal expansion coefficient
- $\mathbf{D} = \mathrm{sym}(\nabla\mathbf{v})$ — stretching tensor
- $\mathbf{W} = \mathrm{skew}(\nabla\mathbf{v})$ — spin tensor
- $\mathbf{I}$ = fourth-order identity tensor
- $\mathbf{1}$ = second-order identity tensor

Summary:

- Stress rate follows Jaumann derivative to ensure frame indifference.
- Elastic response governed by isotropic fourth-order tensor $\mathbb{L}$.
- Thermal expansion introduces additional stress through $\mathbf{\Pi}\dot{\theta}$.

Reference Configuration

Framework in the Reference Configuration

- The free energy ψ is defined relative to the reference configuration.
- State variables like $E^e, \theta, \bar{g}, \bar{\mathbf{B}}, s$ are used as arguments of ψ.
- Stress is expressed using the second Piola–Kirchhoff tensor $\mathbf{S}$.
- Dissipation inequality, stress–strain relations, and evolution laws are all written in reference variables.
- Mass density ρ_0 from the reference configuration normalizes all terms.

Key Equations in the Reference Frame

- Free energy:

$$\boxed{\psi = \psi(E^e, \theta, \bar{g}, \bar{\mathbf{B}}, s)}$$

- Dissipation inequality:

$$\boxed{\dot{\psi} + \eta\dot{\theta} - \rho_0^{-1}\mathbf{S} : \dot{E} + (\rho_0\theta)^{-1}\mathbf{q}_0 \cdot \mathbf{g}_0 \leq 0}$$

- Constitutive relation:

$$\boxed{\mathbf{S} = \rho_0 \frac{\partial\psi}{\partial E^e}}$$

Summary:

- In the reference configuration, all energy storage, stress updates, and internal variable evolution are formulated with reference-frame quantities for consistency and objectivity.

Thermodynamic Separation

1. **Start with Total Dissipation:**

$$\mathcal{D} = \dot{\omega} - \dot{\psi} \geq 0$$

where $\dot{\omega} = \widehat{\mathbf{T}} : \dot{\mathbf{E}}^e + (\mathbf{C}^e \widehat{\mathbf{T}}) : \mathbf{L}^p$

2. **Split Stress Power:**

$$\dot{\omega} = \dot{\omega}^e + \dot{\omega}^p$$

with:
- $\dot{\omega}^e = \widehat{\mathbf{T}} : \dot{\mathbf{E}}^e$
- $\dot{\omega}^p = (\mathbf{C}^e \widehat{\mathbf{T}}) : \mathbf{L}^p$

3. **Group Terms with $\dot{\psi}$:**

$$(\dot{\omega}^e - \dot{\psi}) + \dot{\omega}^p \geq 0$$

4. **Apply Elastic Energy Consistency:**

$$\dot{\omega}^e - \dot{\psi} = 0 \quad \Rightarrow \quad \dot{\omega}^p \geq 0$$

Key Physical Insights

- **Elastic deformations** are recoverable and do not cause entropy production.
- **All dissipation** stems from the plastic flow: $\dot{\omega}^p$.
- **Plastic work** increases entropy and governs viscoplastic evolution.

Summary:
The stress power split ensures that the second law is satisfied by assigning dissipation solely to irreversible processes.

Stress Evolution and Thermal Effects

In the stress evolution equation,

$$\overset{\triangledown}{\mathbf{T}} = \mathbb{L}\left[\mathbf{D} - \mathbf{D}^p\right] - \mathbf{\Pi}\dot{\theta},$$

the term $\mathbf{\Pi}\dot{\theta}$ represents the stress change that would occur due to pure thermal expansion alone, without any mechanical loading.

Why Subtract the Thermal Term?

- Thermal expansion creates strain even without external forces.
- Without subtracting $\mathbf{\Pi}\dot{\theta}$, the model would falsely attribute thermal strain as mechanical stress.
- Subtracting isolates the true mechanical response from thermal effects.

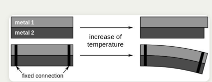

Summary:
- Thermal expansion induces strain without force.
- Subtracting $\mathbf{\Pi}\dot{\theta}$ ensures only mechanical strains generate stresses.
- This keeps the constitutive model physically accurate during heating and cooling.

Relaxed (Intermediate) Configuration

Context for the Relaxed Configuration

- The relaxed configuration represents the material after removing plastic deformations but before applying new elastic deformations.
- It is introduced to separate permanent plastic effects from recoverable elastic effects.
- All thermodynamic potentials, internal variables, and evolution laws are defined relative to this frame.
- The relaxed state provides a clean, natural reference for measuring elastic strain E^e and computing dissipation.

What Happens in the Relaxed Configuration?

- The elastic deformation gradient F^e is measured from the relaxed state to the current deformed state.
- Elastic strain measures like C^e and E^e are defined in this configuration.
- The Kirchhoff stress $\tilde{\mathbf{T}}$ is naturally associated with the relaxed volume.
- Plastic flow is accounted for separately through the plastic velocity gradient $\mathbf{L}^p$.

Summary:

- The relaxed configuration isolates elastic responses cleanly, enabling proper definition of thermodynamics and plastic evolution laws.

Relaxed Configuration Constituative Laws

Kinematics in the Relaxed Configuration

- Elastic deformation gradient:

$$F = F^e F^p \quad \Rightarrow \quad F^e = F F^{p-1}$$

- Elastic right Cauchy-Green tensor:

$$C^e = F^{eT} F^e$$

- Elastic Green–Lagrange strain tensor:

$$E^e = \frac{1}{2}(C^e - I)$$

Stress and Power Quantities

- Kirchhoff stress (weighted Cauchy stress):

$$\tilde{\mathbf{T}} = (\det F)\mathbf{T}$$

- Stress power split:

$$\dot{\omega} = \dot{\omega}^e + \dot{\omega}^p$$

$$\dot{\omega}^e = \tilde{\mathbf{T}} : \dot{E}^e \quad , \quad \dot{\omega}^p = (C^e \tilde{\mathbf{T}}) : \mathbf{L}^p$$

Summary:

- Elastic kinematics and stress measures are formulated relative to the relaxed configuration, cleanly separating plastic and elastic contributions.
- Stress Power Split allows Anand to cleanly isolate plastic dissipation from elastic storage.
- Green-Lagrange strain tensor E^e is used because it symmetrically captures nonlinear elastic strain relative to the relaxed configuration
- The right Cauchy-Green tensor $C^e = F^{e^T} F^e$ is required as an intermediate to compute E^e from the elastic deformation gradient F^e without referencing spatial coordinates

5. Energy n=0 Classic

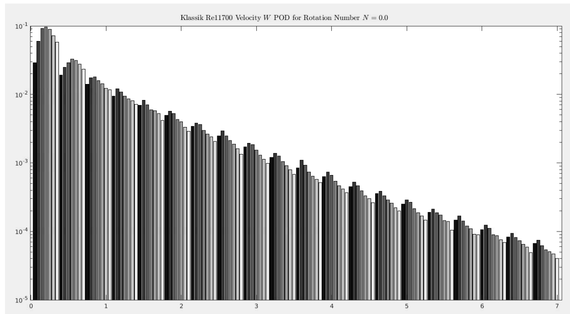

1.3. Important Switches

pipe = Pipe(); creates a Pipe Class. As the functions (above) are called, data is stored in sub-structs:

1. obj.CaseId - stores properties like Re, rotation number S, experimental flags such as quadrature (simpson/trapezoidal), number of gridpoints, frequently called vectors (rMat $r = 1, \ldots, 0.5$)
2. obj.pod - eigen data, used for calculating POD
3. obj.solution - computed POD modes
4. obj.plt - plot configuration

4.4. Klassik POD S=3.0

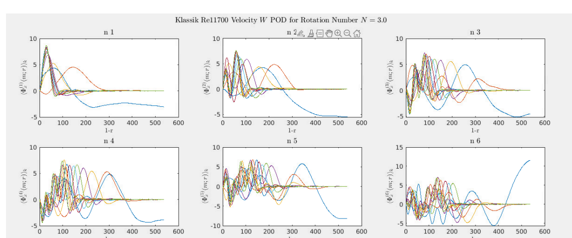

4.3. Klassik POD S=0.0

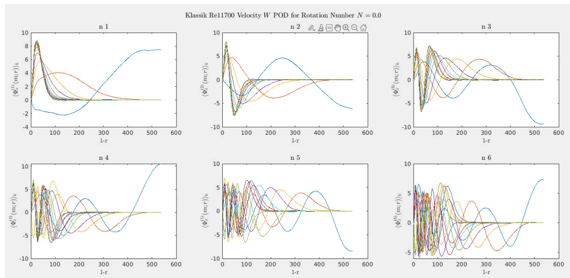

2.1. Classic POD Equations

The following equations are used in the above code.

$$\int_{r'} \mathbf{S}(k;m;r,r')\,\Phi^{(n)}(k;m;r')\,r'\mathrm{d}r' = \lambda^{(n)}(k;m)\Phi^{(n)}(k;m;r)$$

$$\mathbf{S}(k;m;r,r') = \lim_{T\to\infty}\frac{1}{T}\int_0^T \mathbf{u}(k;m;r,t)\mathbf{u}^*(k;m;r',t)\,\mathrm{d}t$$

$$\alpha^{(n)}(k;m;t) = \int_r \mathbf{u}(k;m;r,t)\Phi^{(n)^*}(k;m;r)r\,\mathrm{d}r$$

2.2. Classic POD Equations (Fixed)

$$\int_{r'} \underbrace{r^{1/2} S_{i,j}\left(r, r'; m; f\right) r'^{1/2}}_{W_{i,j}(r,r';m;f)} \underbrace{\phi_j^{*(n)}\left(r'; m; f\right) r'^{1/2}}_{\hat{\phi}_j^{\psi(i)}(r';m;f)} \mathrm{d}r'$$

$$= \underbrace{\lambda^{(n)}(m, f)}_{\hat{\lambda}^{(n)}(m;f)} \underbrace{r^{1/2} \phi_i^{(n)}(r; m; f)}_{\hat{\phi}_i^{(n)}(r,m;f)}$$

$$\alpha_n(m;t) = \int_r \mathbf{u}(m;r,t) r^{1/2} \Phi_n^*(m;r) dr$$

4.2. Snapshot-Classic Comparison

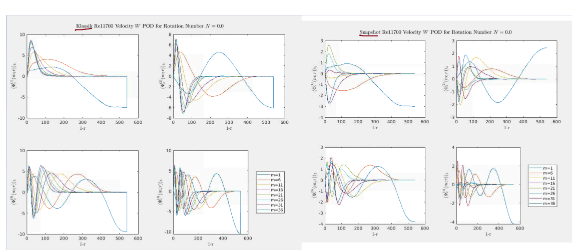

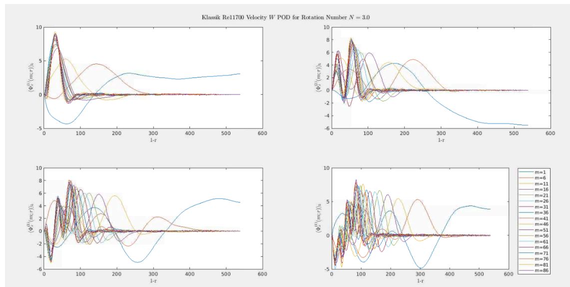

$$\lim_{\tau\to\infty}\frac{1}{\tau}\int_0^{\tau}\mathbf{u}_{\mathrm{T}}(k;m;r,t)\alpha^{(n)^*}(k;m;t)\mathrm{d}t$$
$$=\Phi_{\mathrm{T}}^{(n)}(k;m;r)\lambda^{(n)}(k;m)$$
$$\mathbf{R}\left(k;m;t,t'\right)=\int_r \mathbf{u}(k;m;r,t)\mathbf{u}^*\left(k;m;r,t'\right)r\,\mathrm{d}r$$
$$\lim_{\tau\to\infty}\frac{1}{\tau}\int_0^{\tau}\mathbf{u}_{\mathbf{T}}(k;m;r,t)\alpha^{(n)*}(k;m;t)\,\mathrm{d}t$$
$$=\Phi_{\mathbf{T}}^{(n)}(k;m;r)\lambda^{(n)}(k;m).$$

2.4. Reconstruction

The reconstruction is given by

$$q(\xi, t) - \bar{q}(\xi) \approx \sum_{j=1}^{r} a_j(t)\varphi_j(\xi) \Rightarrow$$
$$q(r, \theta, t; x) = \bar{q}(r, \theta, t; x) + \sum_{n=1}\sum_{m=0} \alpha^{(n)}(m; t)\Phi^{(n)}(r; m; x)$$

Since the snapshot pod implementation is not error-free, the reconstruction can only be recovered by writing for $\texttt{factor} \gg 0$.

$$q(r, \theta, t; x) = \bar{q}(r, \theta, t; x) + (\text{factor } \gamma)\sum_{n=1}\sum_{m=0} \alpha^{(n)}(m; t)\Phi^{(n)}(r; m; x)$$

4. Result Comparison Classic/Snapshot

3.2. 6 Derivation

The cross-correlation tensor $\mathbf{R}$ is defined as $\mathbf{R}\left(k;m;t,t'\right) = \int_r \mathbf{u}(k;m;r,t)\mathbf{u}^*\left(k;m;r,t'\right) r \,\mathrm{d}r$. This tensor is now transformed from $[3r \times 3r']$ to a $[t \times t']$ tensor. The n POD modes are then constructed as,

$$\lim_{\tau \to \infty} \frac{1}{\tau} \int_0^{\tau} \mathbf{u}_{\mathrm{T}}(k;m;r,t)\alpha^{(n)^*}(k;m;t)\mathrm{d}t = \Phi_{\mathrm{T}}^{(n)}(k;m;r)\lambda^{(n)}(k;m).$$

2.5. Reconstruction

In order to reconstruct in code, caseId.fluctuation = 'off'. This is incorrect. The necessary use of (factor γ) is incorrect

3. Derivation

To derive the questioned equation, consider the integral:

$$\frac{1}{\tau}\int_0^\tau \mathbf{u}_\mathrm{T}(k;m;r,t)\alpha^{(n)^*}(k;m;t)dt.$$

Substitute $\mathbf{u}_\mathrm{T}$ with its expansion:

$$\frac{1}{\tau}\int_0^\tau \left(\sum_l \Phi_\mathrm{T}^{(l)}(k;m;r)\alpha^{(l)}(k;m;t)\right)\alpha^{(n)^*}(k;m;t)dt.$$

3.1. 4 Derivation

Exchange the order of summation and integration, and apply orthogonality,

$$\sum_l \Phi_\mathrm{T}^{(l)}(k;m;r)\left(\frac{1}{\tau}\int_0^\tau \alpha^{(l)}(k;m;t)\alpha^{(n)^*}(k;m;t)dt\right).$$

Due to the orthogonality, namely that $\alpha^{(n)}$ and $\alpha^{(p)}$ are uncorrelated

$$\langle a^{(n)}\alpha^{(p)}\rangle = \lambda^{(n)}\delta_{np}$$

all terms where $l \neq n$ will vanish, and there remains only the $l = n$ term,

$$\Phi_\mathrm{T}^{(n)}(k;m;r)\left(\frac{1}{\tau}\int_0^\tau \alpha^{(n)}(k;m;t)\alpha^{(n)^*}(k;m;t)dt\right).$$

This derivation assumes the normalization of modes and their orthogonality, along with the eigenvalue relationship to simplify the original integral into a form that reveals the spatial structure ($\Phi_\mathrm{T}^{(n)}$) of each mode scaled by its significance $\left(\lambda^{(n)}\right)$.

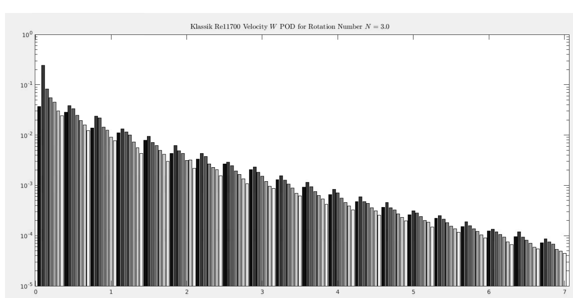
Klassik Re11700 Velocity W POD for Rotation Number N = 3.0
10^0
10^-1
10^-2
10^-3
10^-4
10^-5
0
1
2
3
4
5
6
7

6. Reconstruction

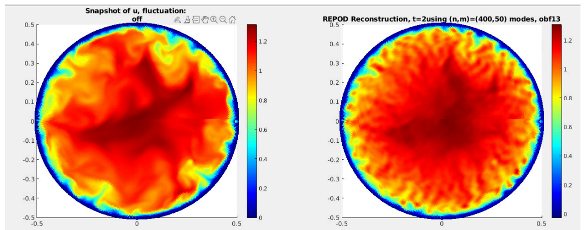
Snapshot of u, fluctuation: off
REPOD Reconstruction, t=2using (n,m)=(400,50) modes, obf13